

## RESEARCH LETTER

10.1002/2014GL060241

## Key Points:

- MJO influences probability of extreme rainfall over southeast Asia
- A seasonal forecast system reproduces the influence and shows prediction skills
- Prediction of extreme events will help preparedness

## Supporting Information:

- Readme
- Text S1 and Figures S1–S5

## Correspondence to:

P. Xavier,  
prince.xavier@metoffice.gov.uk

## Citation:

Xavier, P., R. Rahmat, W. K. Cheong, and E. Wallace (2014), Influence of Madden-Julian Oscillation on Southeast Asia rainfall extremes: Observations and predictability, *Geophys. Res. Lett.*, *41*, 4406–4412, doi:10.1002/2014GL060241.

Received 5 MAY 2014

Accepted 5 JUN 2014

Accepted article online 11 JUN 2014

Published online 30 JUN 2014

Corrected 8 SEP 2014

This article was corrected on 27 SEP 2014. See the end of the full text for details.

## Influence of Madden-Julian Oscillation on Southeast Asia rainfall extremes: Observations and predictability

Prince Xavier<sup>1,2</sup>, Raizan Rahmat<sup>1</sup>, Wee Kiong Cheong<sup>1</sup>, and Emily Wallace<sup>2</sup><sup>1</sup>Centre for Climate Research Singapore, Singapore, <sup>2</sup>Met Office Hadley Centre, Exeter, UK

**Abstract** The influence of Madden-Julian Oscillation (MJO) on the rainfall distribution of Southeast Asia is studied using TRMM satellite-derived rainfall and rain gauge data. It is shown that convectively active (suppressed) phases of MJO can increase (decrease) the probability of extreme rain events over the land regions by about 30–50% (20–25%) during November–March season. The influence of MJO on localized rainfall extremes are also observed both in rainfall intensity and duration. The Met Office Global Seasonal forecasting system seasonal forecasting system is shown to reproduce the MJO influence on rainfall distribution well despite the model biases over land. Skills scores for forecasting 90th percentile extreme rainfall shows significant skills for convective phases. This study demonstrates the feasibility of deriving probabilistic forecasts of extreme rainfall at medium range.

## 1. Introduction

The weather and climate over Southeast Asian (SEA) region is heavily influenced by the complex nature of the land-ocean distribution and orography. The large-scale monsoon systems and tropical modes of variability such as the El Niño–Southern Oscillation, the Madden-Julian Oscillation (MJO), and equatorial waves are also known to influence the weather systems over the region. Due to the high vulnerability of the region to extremes (particularly rainfall) due to high population density, low-lying islands, and marine ecosystems [Manton *et al.*, 2001], it is important to have some level of probabilistic information on the occurrence of such extreme rain events for better preparedness at weather time scales through to seasonal time scales.

On intraseasonal time scales (20–90 days), MJO is the dominant mode of tropical intraseasonal variability and is most active in the boreal winter [Madden and Julian, 1994]. The influences of the MJO on the patterns of precipitation in the global tropics and extratropics have been documented in several studies [e.g., Jones *et al.*, 2004]. Due to its slow evolution and large-scale structure, MJO provides predictability at medium range [e.g., Kang and Kim, 2010]. Many of the current generation of General Circulation Models (GCMs) show useful skill in forecasting MJO phases 2–3 weeks ahead [e.g., Matsueda and Endo, 2011; Waliser *et al.*, 2003]. Quantifying the potential influence of MJO on the probability of occurrence of extreme events is therefore a first step toward forecasting the likelihood of such high-impact extreme rain events over the region.

This study examines the impact of MJO on the rainfall probability distribution of SEA using satellite and quality-controlled rain gauge data during convectively active and suppressed MJO phases. This relationship is evaluated in the state-of-the-art Met Office Global Seasonal forecasting system (GloSea5) and the skills in forecasting extremes is computed with the aim of probabilistic prediction of extreme rainfall events at medium range.

## 2. Data and Methods

Tropical Rainfall Measuring Mission (TRMM) 3B42 daily data [Kummerow *et al.*, 2000] is used in this study. 3B42 algorithm produces TRMM-adjusted merged-infrared precipitation and root-mean-square precipitation-error estimates. Rainfall at  $0.25^\circ \times 0.25^\circ$  spatial resolution has been used. Daily wind fields and specific humidity (for moisture budget calculations see supporting information) are obtained from the European Centre for Medium-Range Weather Forecasts ERA-Interim [Dee *et al.*, 2011] reanalysis. Data for the period 1998–2012 are analyzed here. In order to validate the results obtained from TRMM 3B42 data over the land regions gridded data at  $0.25^\circ \times 0.25^\circ$  spatial resolution from Asian Precipitation-Highly-Resolved Observational Data Integration Towards Evaluation of Water Resources (APHRODITE) [Yatagai *et al.*, 2012] data are used for a common period 1998–2007. In order to quantify the MJO influence on much smaller local

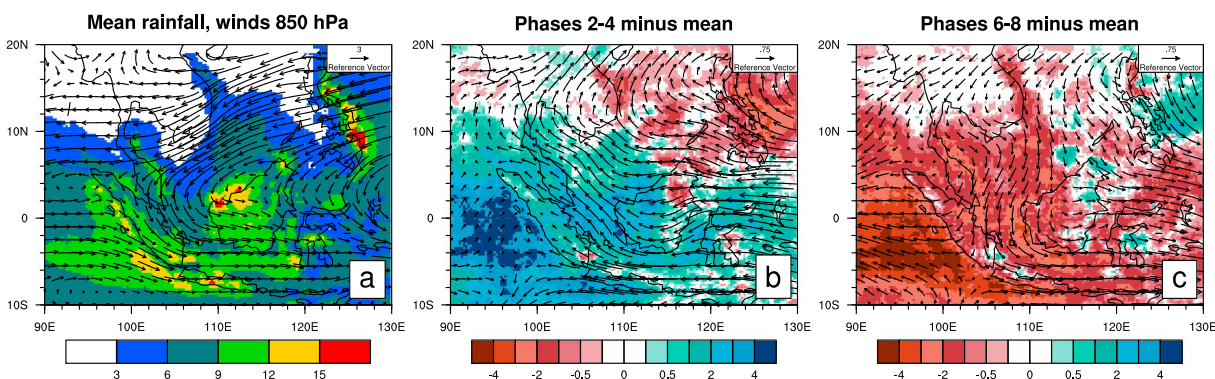


**Figure 1.** (a) Climatological mean rainfall ( $\text{mm d}^{-1}$ ) and 850 hPa winds ( $\text{m s}^{-1}$ ) for NDJFM. Change in rainfall and 850 hPa winds during MJO (b) phases 2–4 and (c) phases 6–8 compared to climatology are also shown.

domains, high-quality rain gauge data from Meteorological Services Singapore from 1980 to 2011 is used (more details on data sets in the supporting information).

MJO dates are identified using the Real-time Multivariate MJO (RMM) Index [Wheeler and Hendon, 2004]. These RMMs are used to define eight MJO phases and amplitude on any given day. MJO convective and suppressed phases are chosen based on the central SEA region including Singapore. During phases 2–4 the MJO’s convective envelope is over this region while during phases 6–8 the convection is over the central and eastern Pacific and the associated suppressed convective activity occurs over the central SEA region. Composites based on these two sets of phases are used in this study.

### 3. MJO Impact on Rainfall Distribution

November to March (hereafter NDJFM) is the primary rainfall season for most countries in the SEA region. Climatological mean rainfall and 850 hPa winds (Figure 1a) for the NDJFM season for the period 1998–2012 shows regions of increased rainfall over the west coast of Sumatra, Malay Peninsula, north of Borneo, and east of Philippines. Winds are predominantly northeasterly over the South China Sea (SCS) and westerlies over the eastern Indian Ocean and SEA is the region of strong low-level convergence with abundance of moisture. NDJFM is also the active MJO season over the region with more eastward propagating events compared to the other seasons [Zhang and Dong, 2004]. MJO composites are constructed for different phases with normalized MJO amplitude greater than 1. Phases 2–4 produce significantly increased rainfall anomalies, and phases 6–8 decreases rainfall over the region (Figure S1). For the convenience of presentation we have combined phases 2–4 as the active convective phase and 6–8 as the suppressed phase (Figures 1b and 1c) over the region. Notable increase occurs over the Sumatra and eastern Indian Ocean and Borneo in phases 2–4 with enhanced easterlies to the east of enhanced precipitation (Figure 1b). The circulation over SCS is anticyclonic and weakens the mean northeasterly flow. This tend to reduce number of northeasterly cold surges during MJO episodes [Chang et al., 2005]. On the other hand, phases 6–8 suppress rainfall and the low-level wind anomalies are predominantly divergent (Figure 1c). The average increase of rainfall over Sumatra and Malay Peninsula in phases 2–4 compared to phases 6–8 is about 3–5  $\text{mm d}^{-1}$  which constitutes about 40–50% of the seasonal mean rainfall.

The changes in probability distribution function (PDF) of rainfall during MJO phases 2–4 and MJO phases 6–8 and when the normalized RMM amplitude is greater than 1 with respect to the climatological PDF (with all days in NDJFM included) are shown in Figure 2. PDFs are represented as box plots with the lower and upper bounds as 5th and 95th percentile values (Figure 2a). PDF of TRMM over land regions are compared with that of APHRODITE. The median values (and mean) of both TRMM over land grid boxes and APHRODITE are comparable, but the PDFs of TRMM land points are more positively skewed compared to that of APHRODITE. PDFs of all ocean grid boxes are also shown for all days case, MJO phases 2–4 and phases 6–8. In all the three sets of box plots, it is clear that MJO phases 2–4 tend to have a more positively skewed rainfall distribution compared to all phases and MJO phases 6–8 have a lower skewness of the PDF.

These differences are highlighted in Figure 2b as percentage changes in rainfall PDFs for land regions between 10°S and 10°N from TRMM and APHRODITE for the SE Asia region. Percentage change in

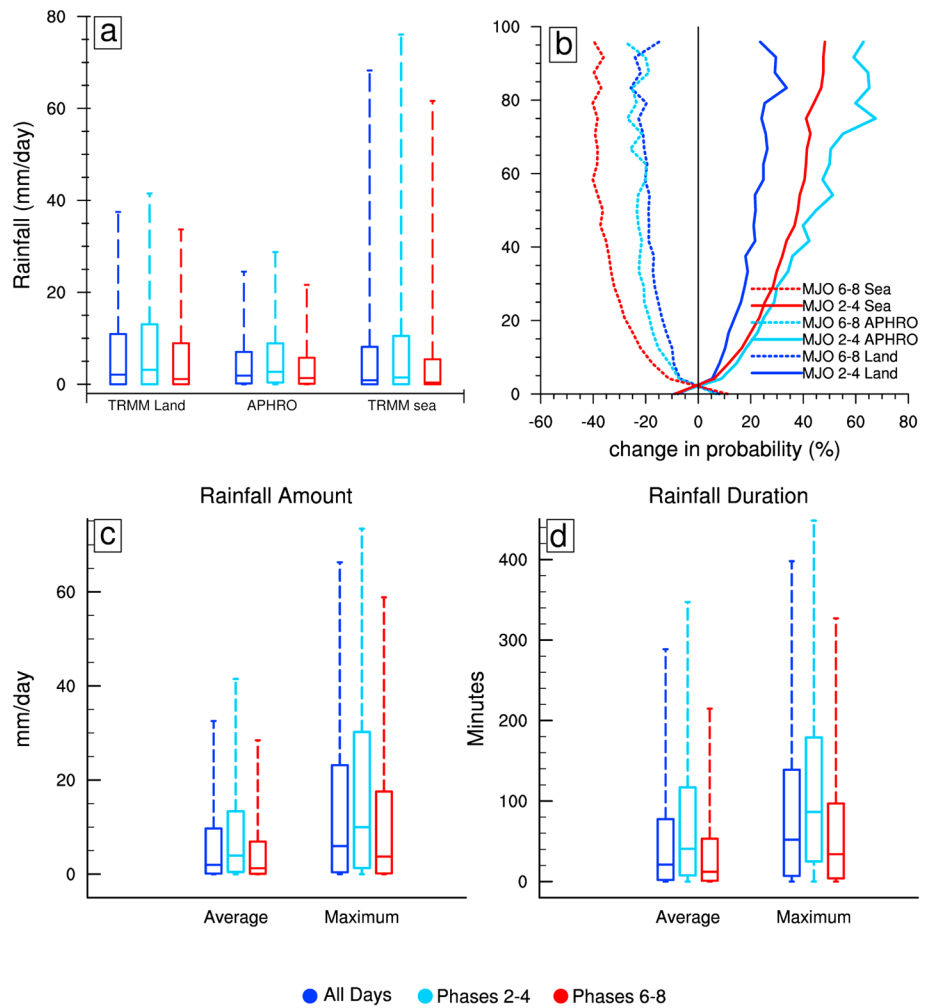


**Figure 2.** (a) PDFs of rainfall for all days (dark blue), MJO phases 2–4 (light blue), and 6–8 (red) from TRMM land points, APHRODITE and TRMM ocean points. (b) Percentage change of probabilities of rainfall for different MJO states with respect to the PDF of all days. All land points between 90°–125°E and 10°S–10° N are used to construct PDFs. (c, d) Daily rainfall amount (in  $\text{mm d}^{-1}$ ) and duration (in minutes) during the NDJFM season for all days, MJO phases 2–4 and MJO phases 6–8 over Singapore. The values depicted on the box plots are the median, the 5th, 25th (lower quartile), 75th (upper quartile), and 95th percentile values. “Average” refers to the daily rainfall values averaged across the five different stations, while “Maximum” refers to the daily rainfall values highest among the five stations recorded on any given day.

probability of rainfall in each bin during phases 2–4 and 6–8 with respect to that of all NDJFM days are plotted. This figure suggests that there is more than 30% increase in probability of moderate to strong land rainfall events during phases 2–4 compared to the normal. There is a much larger increase in the probability of extreme events in APHRODITE (about 60% higher for rainfall bins greater than 60  $\text{mm d}^{-1}$ ). Over the land (both in TRMM and APHRODITE) percentage reduction in probability due to phases 6–8 are fairly similar and is about 20% for moderate and extreme events alike. Similar figures for ocean grid points for the domain are also shown in Figure 2b. Over the ocean, there is a higher probability for nearly all precipitation bins compared to TRMM land points during MJO phases 2–4. Increase in probability due to phases 2–4 and decrease due to phases 6–8 are nearly equal over the ocean points. Moisture budget analysis (see supporting information) shows reduced (enhanced) advective drying of the lower levels may play an important role during phases 2–4 (6–8) in modulating the extreme rainfall events.

This section also examines whether the large-scale signal discussed above are representative of local-scale variability rainfall extremes. Presence of a clear regional signal guarantees that MJO influence is also felt at very local scales and this may have significant implications in the regional weather and extended range forecasts. Singapore is a small region for such a verification and with the availability of high-quality rain gauge

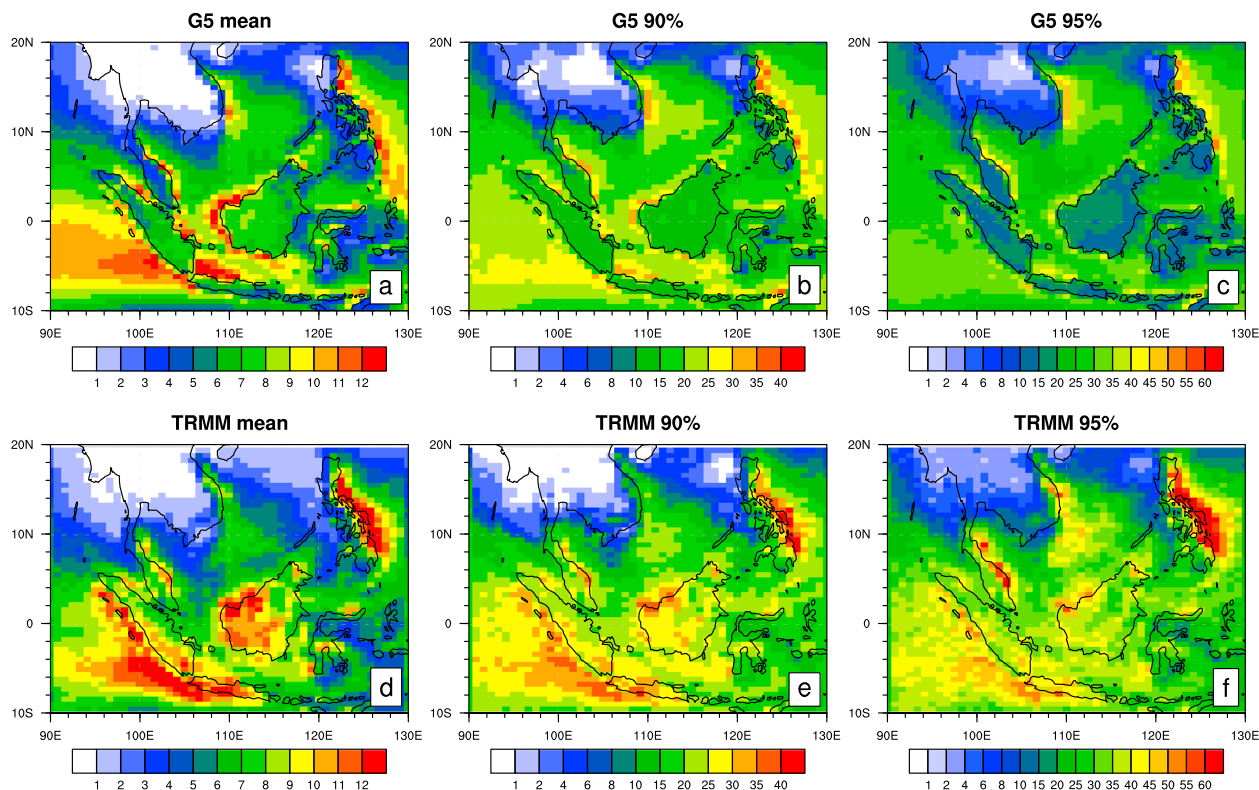


**Figure 3.** Mean rainfall, 90th and 95th percentile values of rainfall ( $\text{mm d}^{-1}$ ) in (a–c) GloSea5 are compared with those from corresponding (d–f) TRMM observations.

data the MJO influence on the local rainfall distribution is examined here. Figures 2c and 2d shows the characteristics of daily rainfall amount (in  $\text{mm d}^{-1}$ ) and duration (in minutes) during the NDJFM season for all days (dark blue), MJO phases 2–4 (light blue), and MJO phases 6–8 (red). The box plots are constructed using data from five-manned rainfall stations distributed over Singapore Island for approximately 26 year period between January 1987 and October 2012. The daily rainfall composites for the different MJO phases (2–4 and 6–8) are derived from the RMM indices [Wheeler and Hendon, 2004]. It is notable from these box plots that the MJO also has significant impacts on the local scale. MJO phases 2–4 results in the rainfall distribution to increase in both the amount and duration, while MJO phases 6–8 cause the opposite. These patterns are evident in both the average and maximum of the rainfall records and are consistent for the different percentile values.

#### 4. Predictability of Extreme Rainfall

One of the objectives of this study is to evaluate the skill of GloSea5 system to reproduce the MJO influence on extreme events. Given that GloSea5 has good skills in forecasting MJO phases, this analysis would help derive probabilistic information of likelihood of extreme events during the passage of MJO phases. Hindcast data for the period 1998–2009 for initial conditions that covers the NDJFM season (25 October, 1 November, 9 November, 25 January, 1 February, and 9 February) are used here. TRMM rainfall has been regridded to the model grid ( $0.83^\circ \times 0.56^\circ$ ) for comparison.

Figure 3 shows the mean DJFM rainfall and the spatial distribution of 90th and 95th percentile values in GloSea5 and TRMM observations. In general the locations of oceanic rainfall variability are well captured in the model. The patterns of rainfall and regional maxima along the coastal regions of eastern Malay Peninsula, northern Borneo, east of Philippines, and western Sumatra have been well represented with high skill (Figures 3a and 3d). However, the land rainfall and the extreme rainfall values in GloSea5 are underestimated.

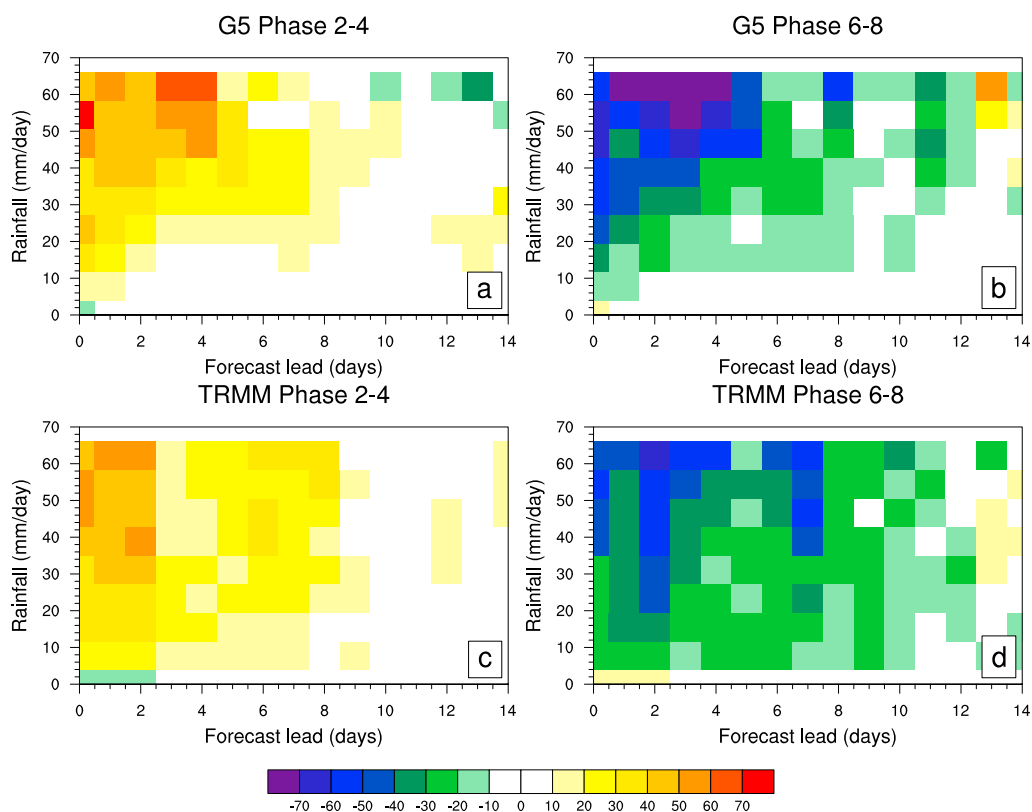


**Figure 4.** Percentage changes in the probability in GloSea5 system when initialized from MJO phases (a) 2–4 and (b) 6–8 with respect to a climatological PDF. (c, d) Verification of these changes from TRMM. Rainfall PDF is computed for a region 90°–120°E, 5°S–10°N.

The skill of the model in forecasting regional extremes is examined in Figures 4a and 4b which shows the percentage change in probability of rainfall when the forecasts are initialized from phases 2–4 and phases 6–8. Verifications from TRMM observations are shown in Figures 4c and 4d. There is about 30–50% increase in the probability of rain events stronger than 20 mm d<sup>-1</sup> in the first 10 days of the forecast which is comparable to the increase seen in TRMM observations (Figure 4c). The suppression of rainfall extremes during phases 6–8 extends up to 12 days. GloSea5 forecasts this suppression well albeit an over estimation of the suppression around 3 day lead. This analysis suggests the potential usefulness of using medium-range forecasts for forecasting the likelihood of extreme rainfall due to MJO. A more robust measure of the forecast skill of extremes, Symmetric Extremal Dependence Index (SEDI) is proposed by *Ferro and Stephenson [2011]* for assessing the skill of deterministic forecasts of rare binary events. *Marshall et al. [2013]* uses SEDI to assess the forecast skill of temperature extremes over Australia. SEDI has been used to assess skills of GloSea5 forecasts of 90th percentile rainfall extremes (more details in the supporting information).

SEDI is based on a 2 × 2 contingency table and is computed using the hit rate (*H*) and false alarm rate (*F*) as

$$SEDI = \frac{\log(F) - \log(H) - \log(1 - F) + \log(1 - H)}{\log(F) + \log(H) + \log(1 - F) + \log(1 - H)} \quad (1)$$

A forecast is counted as a “hit” if it and the corresponding observation both exceed a particular threshold (the 90th percentile in our study); and a “false alarm” if the forecast exceeds the threshold but the observations does not. SEDI scores greater (less) than zero indicate skill better (worse) than for random forecasts [*Marshall et al., 2013*].

SEDI for the region (Figure 5) shows higher skills for oceanic regions compared to land regions, which is related to model biases to forecast the extreme rainfall values over land points (Figure 3). SEDI over most land regions at pentad 1 (SEDI at longer lead times is given in the supporting information) for forecasts initialized at MJO phases 2–4 are between 0.1 and 0.5 which indicates superior forecasts skills over random

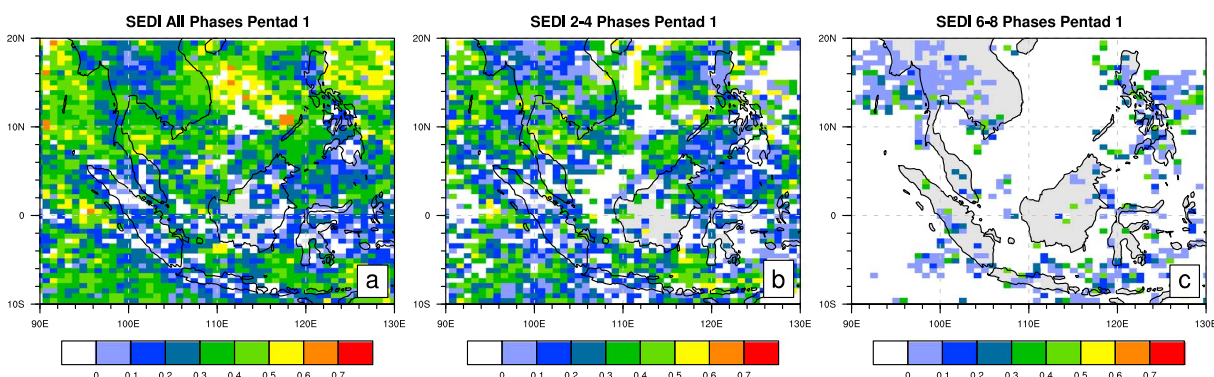


**Figure 5.** SEDI scores for all (a) MJO phases, (b) phases 2–4, and (c) phases 6–8 at the first pentad lead time.

forecasts especially over Malay peninsula, and northern Borneo and Sumatra. The patterns are large scale and indicates the organized large-scale MJO perturbations that are forecasted well by the model. In phases 6–8, however, the skills are much lower given the less organized local convective systems which the model has limited skills to forecast. This is consistent with previous findings that MJO forecasts initialized from a convective phase yields better skills than when they are initialized from convectively inactive phases [e.g., Jones *et al.*, 2000; Goswami and Xavier, 2003]. Some land regions nevertheless show reasonable skills in phases 6–8.

## 5. Conclusions

This study presents evidence that the MJO phases and amplitude modulates the probability and the spatial distribution of rainfall extremes over SEA region. This signal has been shown to be robust using satellite-derived rainfall products, regional rain gauge data, and also using local-scale rainfall data over Singapore. The convective phases of MJO increase the probability of extreme rain events over the land regions by about 30–50% (note the differences in the rainfall PDFs between the satellite-derived rainfall and gauge data in Figure 2). The convectively suppressed phases of MJO (phases 6–8) tend to reduce the probability of precipitation extremes by about 20–25% over land. This is due to changes in the skewness of the precipitation distribution with phases 2–4 (phases 6–8) have more (less) positively skewed distribution compared to the climatological PDF. The influence of MJO on local rainfall extremes are also observed both in the rainfall intensity and the duration. It is also seen that stronger MJO events tend to produce larger increase in the probability of extreme rainfall events (Figure S2). However, for certain regions such as eastern parts of Malaysia and Borneo, the extreme rainfall does not appear to be related to MJO and most likely due to synoptic-scale variability such as cold surges and Borneo vortex. Stronger MJO events tend to have greater influence on extreme rainfall distribution. Moisture budget analysis reveals advective processes may play an important role in the modulation of extreme rainfall due to MJO.

The GloSea5 monthly-seasonal forecasting system shows reasonably high skills up to about 15 days in forecasting MJO. Evaluation of the GloSea5 system in representing the MJO influence on extremes shows GloSea5 reproduces MJO influence on extreme rainfall probabilities well. SEDI skill scores show reasonable forecast skills of 90th percentile rainfall extremes in phases 2–4 compared to phases 6–8. This information on the changes in probabilities of extreme rainfall is highly relevant for the region and future research will look at the forecast skills in more detail so that additional forecasting products based on these probabilities may be derived for the region. This can help better preparedness against such high-impact weather extremes.

### Acknowledgments

Met Office proportion of Prince Xavier's funding is supported by the Joint DECC/Defra Met Office Hadley Centre Climate Programme (GA01101). Authors acknowledge useful comments from Chris Gordon. Craig MacLachlan is acknowledged for making GloSea5 data available. Authors thank Andrew Marshall for providing details of SEDI computation.

The Editor thanks two anonymous reviewers for their assistance in evaluating this paper.

### References

- Chang, C.-P., P. A. Harr, and H.-J. Chen (2005), Synoptic disturbances over the equatorial South China Sea and Western Maritime Continent during Boreal Winter, *Mon. Weather Rev.*, *133*(3), 489–503, doi:10.1175/MWR-2868.1.
- Dee, D., et al. (2011), The ERA-Interim reanalysis: Configuration and performance of the data assimilation system, *Q. J. R. Meteorol. Soc.*, *137*(656), 553–597.
- Ferro, C. A., and D. B. Stephenson (2011), Extremal dependence indices: Improved verification measures for deterministic forecasts of rare binary events, *Weather Forecasting*, *26*, 699–713.
- Goswami, B. N., and P. K. Xavier (2003), Potential predictability and extended range prediction of Indian summer monsoon breaks, *Geophys. Res. Lett.*, *30*(18), 1966, doi:10.1029/2003GL017810.

- Jones, C., D. E. Waliser, J.-K. E. Schemm, and W. K. M. Lau (2000), Prediction skill of the Madden and Julian Oscillation in dynamical extended range forecasts, *Clim. Dyn.*, *16*, 273–289.
- Jones, C., D. E. Waliser, K. Lau, and W. Stern (2004), Global occurrences of extreme precipitation and the Madden-Julian Oscillation: Observations and predictability, *J. Clim.*, *17*(23), 4575–4589.
- Kang, I.-S., and H.-M. Kim (2010), Assessment of MJO predictability for boreal winter with various statistical and dynamical models, *J. Clim.*, *23*(9), 2368–2378.
- Kummerow, C., et al. (2000), The status of the Tropical Rainfall Measuring Mission (TRMM) after two years in orbit, *J. Appl. Meteorol.*, *39*(12), 1965–1982.
- Madden, R. A., and P. R. Julian (1994), Observations of the 40-50-day tropical oscillation—A review, *Mon. Weather Rev.*, *122*(5), 814–837.
- Manton, M., et al. (2001), Trends in extreme daily rainfall and temperature in Southeast Asia and the South Pacific: 1961–1998, *Int. J. Climatol.*, *21*(3), 269–284.
- Marshall, A., D. Hudson, M. Wheeler, O. Alves, H. Hendon, M. Pook, and J. Risbey (2013), Intra-seasonal drivers of extreme heat over Australia in observations and POAMA-2, *Clim. Dyn.*, 1–23, doi:10.1007/s00382-013-2016-1.
- Matsueda, M., and H. Endo (2011), Verification of medium-range MJO forecasts with TIGGE, *Geophys. Res. Lett.*, *38*, L11801, doi:10.1029/2011GL047480.
- Waliser, D. E., K. M. Lau, W. Stern, and C. Jones (2003), Potential predictability of the Madden-Julian Oscillation, *Bull. Am. Meteorol. Soc.*, *84*, 33–50.
- Wheeler, M. C., and H. H. Hendon (2004), An all-season real-time multivariate MJO Index: Development of an index for monitoring and prediction, *Mon. Weather Rev.*, *132*, 1917–1932.
- Yatagai, A., K. Kamiguchi, O. Arakawa, A. Hamada, N. Yasutomi, and A. Kito (2012), APHRODITE: Constructing a long-term daily gridded precipitation dataset for Asia based on a dense network of rain gauges, *Bull. Am. Meteorol. Soc.*, *93*(9), 1401–1415.
- Zhang, C., and M. Dong (2004), Seasonality in the Madden-Julian oscillation, *J. Clim.*, *17*(16), 3169–3180.

## Erratum

In the originally published version of this article, there was a typographical error in Equation (1). The equation has since been corrected and this version may be considered the authoritative version of record.

In Equation (1),  $\log(1 + H)$  has been replaced by  $\log(1 - H)$ .